Langmuir

ARTICLE

pubs.acs.org/Langmuir

CO_2 Adsorption Studies on Hydroxy Metal Carbonates $M(CO_3)_x(OH)_y$ (M = Zn, Zn−Mg, Mg, Mg−Cu, Cu, Ni, and Pb) at High Pressures up to 175 bar

Ferdi Karadas,[†] Cafer T. Yavuz,[‡] Sonia Zulfiqar,[‡] Santiago Aparicio,[§] Galen D. Stucky,[∥] and Mert Atilhan*[,†]

[†]Department of Chemical Engineering, Qatar University, 2713 Doha, Qatar

[‡]Graduate School of EEWS, KAIST, 373−1 Guseong Dong, Yuseong Gu, Daejeon 305-701, Republic of Korea

[§]Department of Chemistry, University of Burgos, 09001 Burgos, Spain

[∥]Department of Chemistry and Biochemistry, University of California—Santa Barbara, Santa Barbara, California, 93106, United States

Supporting Information

ABSTRACT: Carbon dioxide (CO_2) adsorption capacities of several hydroxy metal carbonates have been studied using the state-of-the-art Rubotherm sorption apparatus to obtain adsorption and desorption isotherms of these compounds up to 175 bar. The carbonate compounds were prepared by simply reacting a carbonate (CO_3^{2-}) solution with solutions of Zn^{2+}, Zn^{2+}/Mg^{2+}, Mg^{2+}, Cu^{2+}/Mg^{2+}, Cu^{2+}, Pb^{2+}, and Ni^{2+} metal ions, resulting in hydroxyzincite, hydromagnesite, mcguinnessite, malachite, nullaginite, and hydrocerussite, respectively. Mineral compositions are calculated by using a combination of powder XRD, TGA, FTIR, and ICP-OES analysis. Adsorption capacities of hydroxy nickel carbonate compound observed from Rubotherm magnetic suspension sorption apparatus has shown highest performance among the other components that were investigated in this work (1.72 mmol CO_2/g adsorbent at 175 bar and 316 K).

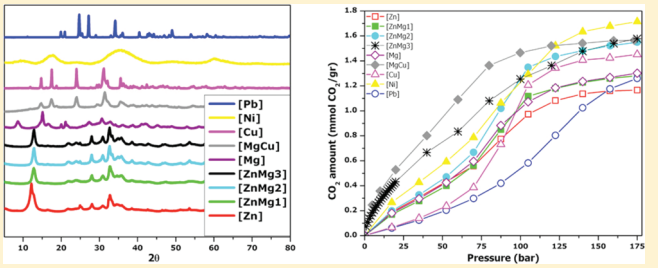

1. INTRODUCTION

Carbon dioxide capture and sequestration (CCS) is becoming increasingly significant owing to the fact that it is one the main greenhouse gases contributing to global warming.[1−5] Since the use of fossil fuels such as natural gas, coal, and petroleum resulted in a substantial increase in CO_2 emission, with approximately 80% percent increase from 1970 to 2005, research has focused on the separation of CO_2 from flue gases via several methods, such as absorption with liquids (e.g., amine solvents and ionic liquids),[6,7] adsorption with porous solids,[8−10] cryogenic distillation, and membrane purification.[11] Of these, porous materials, particularly zeolites, activated carbons, silica-based mesoporous materials, and metal−organic frameworks have received attention due to their promising gas adsorption properties and their easy modification.[8,12−18] Although CO_2 adsorption studies have been performed widely at ambient pressures and at low pressures, there are only a number of studies focusing on their CO_2 capture performance at high pressures.[19] Since carbon dioxide could be removed from flue gases in three different ways—(a) precombustion, (b) postcombustion, and (c) oxy-fuel—each of which possesses distinct requirements and limitations,[20,21] a detailed investigation of promising materials including both high and low pressures is required to analyze the CO_2 capture capacity of these materials. For this reason, Cavenati et al.[22] measured the CO_2 adsorption capacity of Zeolite 13X up to 32 bar at 298 K while Dreisbach et al.[23] measured that of activated carbon Norit R1 extra at 298 K up to 60 bar. Furthermore, metal−organic frameworks such as MIL-101, MOF-177, and IRMOF-1 have been measured up to around 35 bar.[24]

Metal carbonate solutions have also been studied in CO_2 capture. Sodium carbonate solution has been shown to achieve greater than 90% capture of CO_2 when the system is operated for a total of 235 h using fossil-fuel-derived flue gas.[25] Aqueous alkali hydroxide solutions have also been studied to capture CO_2 from air.[26] Herein we investigated the CO_2 adsorption capacity of hydroxy metal carbonate mineral compounds given their stability at extreme conditions and the fact that carboxyl and hydroxyl groups present in their structures have well-known affinities toward CO_2 molecule. Reactions of carbonate with Zn^{2+}, Zn^{2+}/Mg^{2+} mixture, Mg^{2+}, Cu^{2+}/Mg^{2+} mixture, Cu^{2+}, Ni^{2+}, and Pb^{2+} have been performed in this study to obtain hydroxy metal carbonate samples. The prepared samples have then been characterized and studied with the Rubotherm magnetic suspension balance (MSB) to measure the CO_2 adsorption at four different temperatures (316, 325, 334, and 343 K) up to 175 bar.

Received: April 28, 2011
Revised: July 25, 2011
Published: August 01, 2011

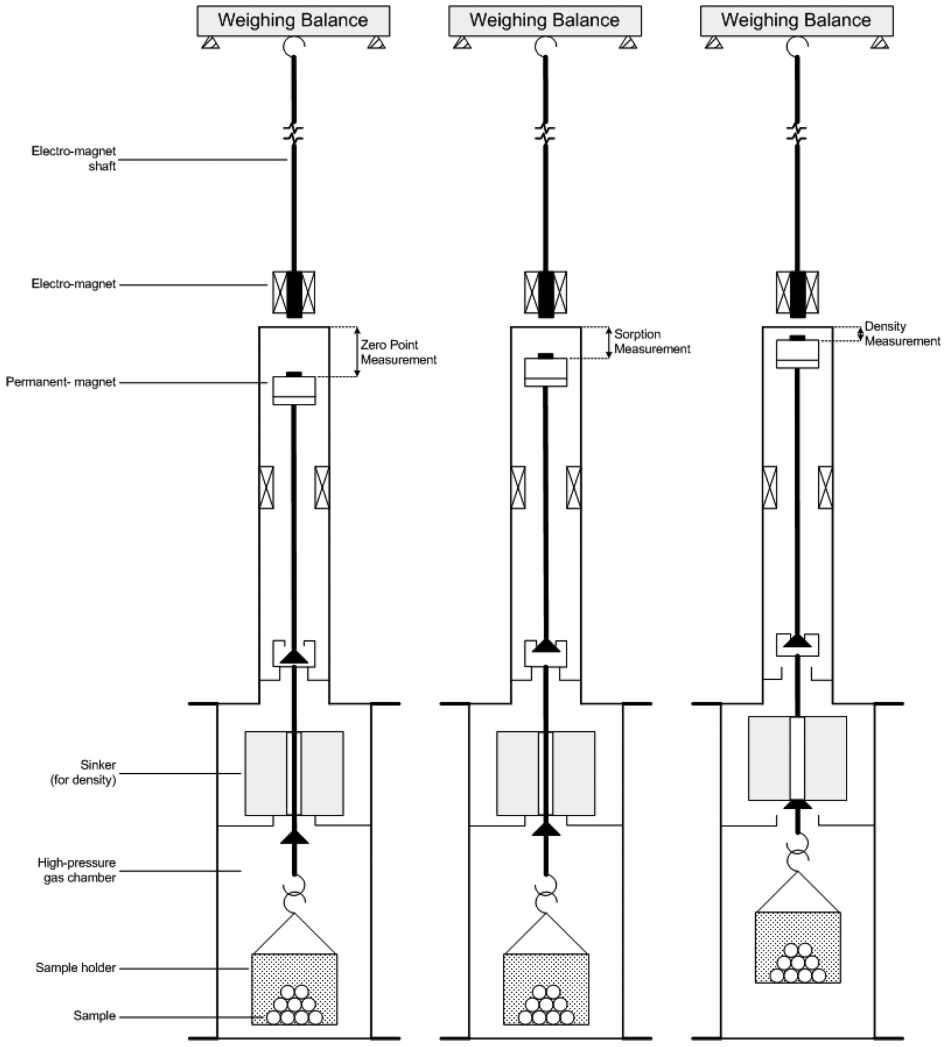

Figure 1. Schematics of MSB and its operation positions used for sorption and density measurements.

2. EXPERIMENTAL SECTION

2.1. Synthesis. The starting materials $ZnCl_2$, $MgCl_2$, $Cu(NO_3)_2$, $Ni(NO_3)_2$, $Pb(CH_3COO)_2$, K_2CO_3, and NaOH were purchased from Aldrich and used as received.

Hydroxy metal carbonates are abbreviated as [**M**] [M = Zn, Mg, Cu, CuMg (for bimetallic copper−magnesium carbonate), Pb, and Ni] throughout the text. [**ZnMg-1**], [**ZnMg-2**], and [**ZnMg-3**] refer to hydroxy zinc−magnesium carbonate compounds with different Zn:Mg stoichiometric ratio.

In a typical synthesis, hydroxy zinc carbonate was prepared by adding a solution of zinc chloride salt (1.34 g, 0.01 mol) in H_2O (20 mL) dropwise to a colorless solution of K_2CO_3 (1.38 g, 0.01 mols) in H_2O (20 mL). The solution was heated to 60 °C and the pH of the solution was maintained at 10 by dropwise addition of 1.0 M NaOH solution. The solution was then allowed to stir overnight. The white precipitate was collected by filtration and rinsed with copious amount of distilled water. The supernatant was tested for Cl^- using 0.1 M $AgNO_3$ solution periodically. The product was dried at 100 °C in an oven for 24 h and stored in glass vials. For [Zn], yield = 1.92 g (87%). Compounds [**Mg**], [**ZnMg-1**], [**ZnMg-2**], [**ZnMg-3**], [**Cu**], [**CuMg**], [**Ni**], and [**Pb**] were prepared in an analogous fashion to that described above for compound [**Zn**]. The yields were 1.82 g (72%), 1.64 g (77%), 1.84 g (79%), 2.11 g (92%), 1.64 (67%), and 1.85 g (86%), respectively.

2.2. Physical Measurements. IR spectra were measured as powder samples on a Perkin-Elmer Spectrum 400 FT-IR spectrometer. The contents of metals in Zn−Mg and Cu−Mg carbonates and the solid phases were determined by ICP-OES using a Varian instrument. For ICP-OES analysis, the solid samples were analyzed after dissolving and acidifying them in a concentrated nitric acid; this dilution was recorded by a balance, and 20 mg of solid was dissolved in 60 g of 0.5 M HNO_3. Internal standards were prepared from ICP quality (Merck) multi-element standard solutions of Cu, Mg, and Zn. Thermal analysis was performed using a Perkin-Elmer Pyris 6 TGA instrument. TGA measurements were made at 10 °C/min from 30 to 600 °C under N_2 on all synthesized samples. The diffraction patterns of powdered samples were recorded using a Rigaku (D/Max-2500) HR-X-ray diffractometer at 40 kV and 300 mA. Measurements were performed for 2θ in the range of 5° to 80° with a step size of 0.01° and scan speed of 2°/min.

2.3. Sorption Measurements. For carbon dioxide adsorption measurements, a high-pressure magnetic suspension balance (MSB) sorption device made by Rubotherm Präzisionsmesstechnik GmbH was used. The MSB apparatus is rated up to 350 bar at 100 °C and it has two different operation positions. First, the measurement cell is filled with the gas, in our case it is carbon dioxide, and at the sorption measurement position, MSB records the weight change of the sample as the high pressure gas is adsorbed by the sample that is placed in the sample

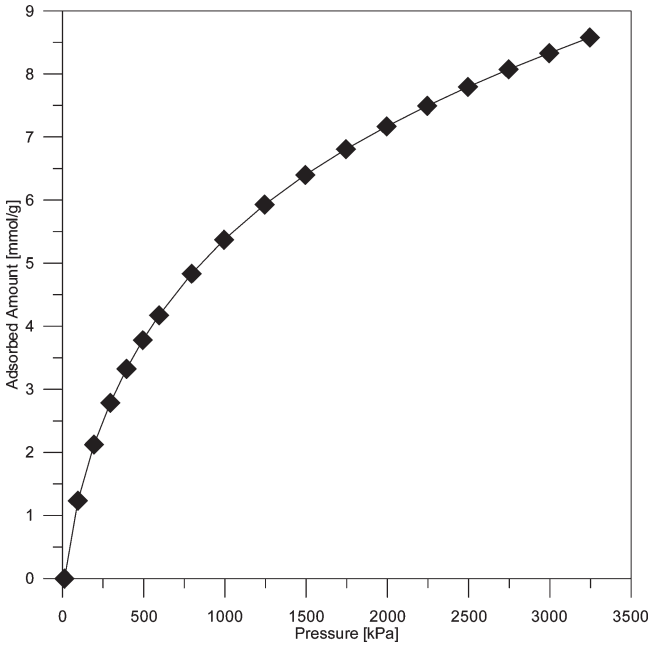

Figure 2. Experimental data for CO_2 adsorption on Norit RB3 (in close agreement with Dreisbach et al.[23]).

holder. The second measurement position is used to measure the in situ density of the high-pressure gas, as it is required to calculate the amount of the adsorbed gas on the solid sample in the high-pressure cell. Figure 1 shows the schematics of the MSB and its operating positions.

MSB measures the change of weight of a sorbent sample in the gravity field due to adsorption of molecules from a surrounding gas phase through the contactless force transmission method, which enables much stable operations at high pressures. The weight gained by the sample within the high-pressure cell is transmitted via contactless method by using magnetic suspension coupling from a closed and pressure-proof metal container to an external microbalance.[27]

The measurement cell is equipped with platinum resistance thermometer Jumo DMM 5017 Pt100 that records temperature of the measuring cell within ±0.6 °C accuracy. Pressure is monitored via Paroscientific Digiquartz 745-3K with an accuracy of 0.01% in pressure in full scale.

Typical measurements start by placing approximately 0.25 g of sample of interest within the sample holder. First the system is taken under vacuum for 24 h at 60 °C. Carbon dioxide is then pressurized via a Teldyne Isco 260D fully automated gas booster and charged into the high-pressure cell and then carbon dioxide adsorption on the sample begins. For each pressure point it takes about 45 min to reach equilibrium (pressure and temperature) and once equilibrium is reached, four different sets of measurements are taken for a period of 10 min; a data point is collected every 30 s. The total duration of each temperature and pressure point takes about 50 min. At the end of each pressure point, the system goes to the next pressure measurement point automatically. In this work, 175 bar is used for the maximum pressure and at the end of each isotherm, a hysteresis check is conducted at each isotherm by collecting desorption data as the system is depressurized.

Adsorption data is analyzed and the amount of adsorbed carbon dioxide on the sample is calculated by using the equation below

$$W + W_{\text{buoy, sample}} + W_{\text{buoy, sink}} = m_{\text{ads}} + m_{\text{sample}} + m_{\text{sink}} \quad (1)$$

where W = the ignal read by the instrument, $W_{\text{buoy,sample}} = V_{\text{sample}} d_{\text{gas}}$ = the buoyancy correction due to sample, V_{sample} = the volume of the sample, d_{gas} = the density of the gas, $W_{\text{buoy,sink}} = V_{\text{sinker}} d_{\text{gas}}$ = the buoyancy correction due to the sinker, V_{sinker} = the volume of the sinker, m_{ads} = the adsorption amount, m_{sample} = the mass of the sample, m_{sink} = the mass of the sinker.

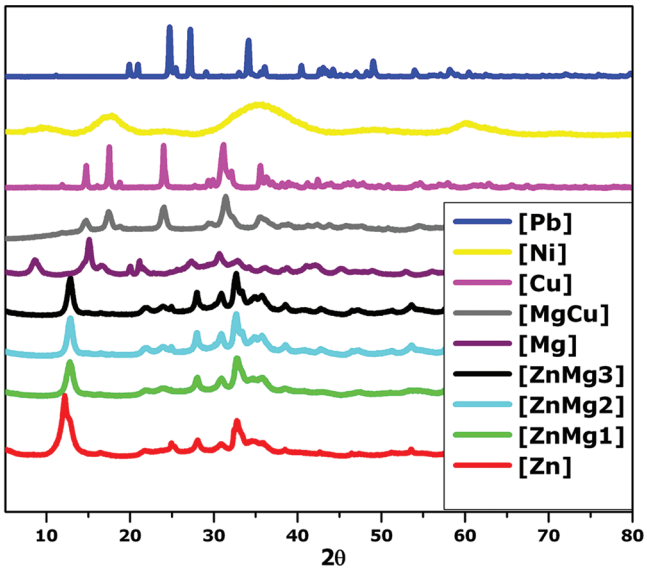

Figure 3. Powder X-ray diffraction (PXRD) patterns of hydroxy metal carbonate compounds.

The d_{gas} is measured in situ by means of the second measurement position (Figure 1). The mass of the empty sinker was measured at several pressures of helium to determine the buoyancy due to the sinker ($W_{\text{buoy,sink}}$). The volume of the sinker (V_{sinker}) is calculated from the slope of weight vs density plot obtained from this measurement. A blank measurement at vacuum was performed to determine the mass of the sinker (m_{sink}).

The buoyancy correction due to the sample ($W_{\text{buoy,sample}}$) was determined by calculating the volume of the sample (V_{sample}) from the crystallographic density of the metal carbonate.[28] The mass of the sample is determined by performing a measurement at vacuum.

Before testing the materials that were synthesized specifically for this work, an activated carbon (Norit RB3) purchased from Sigma-Aldrich was selected as previously tested material in order to ensure the performance of the MSB. Figure 2 shows the Norit RB3 measurement where results match closely with the literature data.

3. RESULTS AND DISCUSSION

3.1. Synthesis and Characterization of Metal Carbonates.

Metal carbonate samples were synthesized by a conventional precipitation method. Solutions with different metal ion molar ratios ([Zn]:[Mg] 6:1, 5:1, 4:1 and [Mg]:[Cu] 3:1) have been slowly added to carbonate solution at constant pH (pH = 10) and temperature (T = 80 °C) to prepare the bimetallic carbonates [**ZnMg-1**], [**ZnMg-2**], [**ZnMg-3**], and [**MgCu**], respectively. The precipitate was then filtered and the powder was dried at 100 °C. The structures of these samples have been investigated with powder X-ray diffraction analysis. Although several other experiments with different metal ion ratios have been performed, since the XRD analysis showed the presence of mixtures of minerals, these results have not been discussed here. Powder X-ray diffraction patterns displayed in Figure 3 show that [**Zn**], [**ZnMg-1**], [**ZnMg-2**], and [**ZnMg-3**] match that of hydrozincite $[Zn_5(CO_3)_2(OH)_6]$,[29] while XRD profiles of [**Mg**], [**MgCu**], [**Cu**], [**Pb**], and [**Ni**] carbonates match to those of hydromagnesite

Table 1. Compounds and Their Corresponding Minerals Obtained by Powder X-ray Diffraction Analysis

compound	corresponding mineral	molecular formula
[**Zn**]	hydrozincite	$Zn_5(CO_3)_2(OH)_6$
[**ZnMg-1**][a]	hydrozincite	$Zn_{4.286}Mg_{0.714}(CO_3)_2(OH)_6$
[**ZnMg-2**][a]	hydrozincite	$Zn_{4.17}Mg_{0.83}(CO_3)_2(OH)_6$
[**ZnMg-3**][a]	hydrozincite	$Zn_4Mg_1(CO_3)_2(OH)_6$
[**Mg**]	hydromagnesite	$Mg_5(CO_3)_4(OH)_2.4H_2O$
[**MgCu**][a]	mcguinnessite	$Mg_{1.5}Cu_{0.5}(CO_3)(OH)_2$
[**Cu**]	malachite	$Cu_2(CO_3)(OH)_2$
[**Ni**]	nullaginite	$Ni_3(CO_3)_2(OH)_2$
[**Pb**]	hydrocerussite	$Pb_2(CO_3)(OH)_2$

[a] The metal content was determined by ICP-OES analysis.

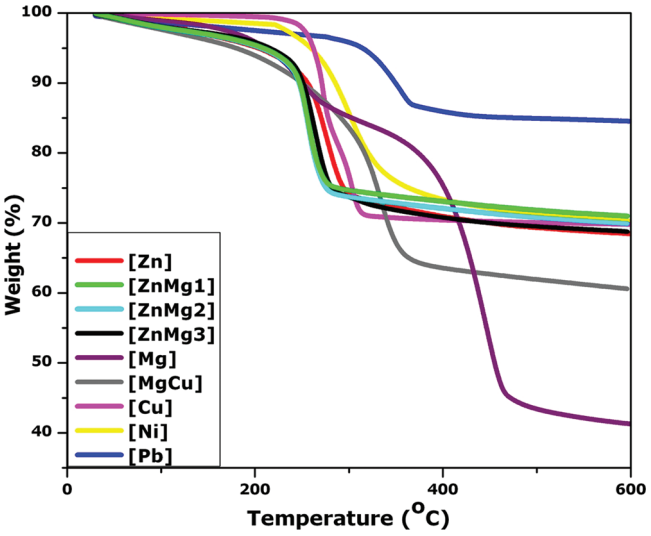

Figure 4. TGA profiles of hydroxy carbonate minerals.

$[Mg_5(CO_3)_4(OH)_2\cdot 4H_2O]$,[30] mcguinnessite $[Mg_{1.5}Cu_{0.5}(CO_3)(OH)_2]$,[31] malachite $[Cu_2(CO_3)(OH)_2]$,[32] hydrocerussite $[Pb_2(CO_3)(OH)_2]$,[33] and nullaginite $[Ni_3(CO_3)_2(OH)_2]$,[34] respectively. The broad Bragg peaks for [**Ni**] could be attributed to the low symmetry of the crystal structure or from a structure that has a large fraction of defects, which is commonly observed for nullaginite minerals. No diffraction peaks characteristic of other solids were detected in the XRD patterns, indicating that the mentioned basic metal carbonates are the only product precipitated. The metal contents of the samples have further been confirmed with ICP-OES analysis (Table 1).

The presence of carbonate and hydroxyl groups has been confirmed with infrared spectra studies. Hydrozincite samples [**Zn**], [**ZnMg-1**], [**ZnMg-2**], and [**ZnMg-3**] are characterized by two intense bands at 1367, 1502 cm^{-1} for [**Zn**], 1369, 1506 cm^{-1} for [**ZnMg-1**], 1365, 1505 cm^{-1} for [**ZnMg-2**], and 1370, 1505 cm^{-1} for [**ZnMg-3**], which are in good agreement with the previously reported results.[29] Each compound also exhibit a broad peak at 3392, 3401, 3381, and 3372 cm^{-1}, respectively, due to the presence of hydroxyl functional groups. For [**Mg**], the bands at 1342, 1401, and 1512 cm^{-1} are attributed to asymmetric C═O stretching vibrations of carbonate molecule, whereas the broad bands at 3384, 3228, and 3139 cm^{-1} are ascribed to the hydroxyl functional group and water content. [**MgCu**] exhibits

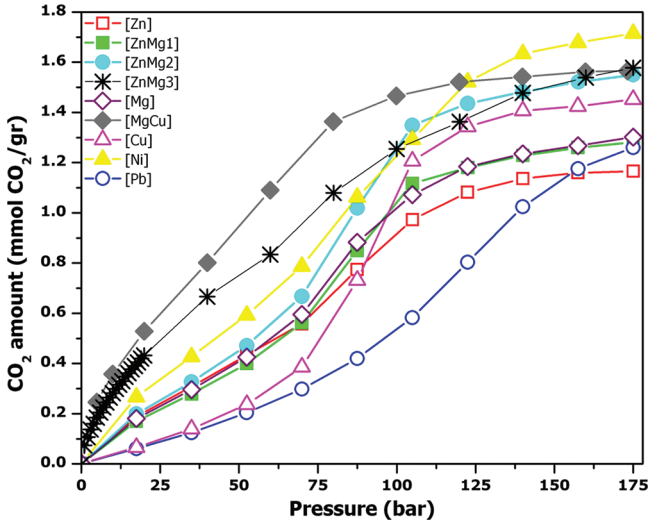

Figure 5. CO_2 adsorption isotherms of compounds at 316 K (43 °C) up to 175 bar.

Table 2. Amount of CO_2 Adsorption (mmol/g adsorbent) at 43 °C

	CO_2 Adsorption (mmol/g) at 43 °C	
compd	P = 35 bar	P = 175 bar
$Zn_5(CO_3)_2(OH)_6$	0.31	1.17
$Zn_{4.286}Mg_{0.714}(CO_3)_2(OH)_6$	0.28	1.28
$Zn_{4.17}Mg_{0.83}(CO_3)_2(OH)_6$	0.33	1.55
$Zn_4Mg_1(CO_3)_2(OH)_6$	0.4	1.60
$Mg_5(CO_3)_4(OH)_2.4H_2O$	0.61	1.58
$Mg_{1.5}Cu_{0.5}(CO_3)(OH)_2$	0.74	1.56
$Cu_2(CO_3)(OH)_2$	0.14	1.45
$Ni_3(CO_3)_2(OH)_2$	0.43	1.72
$Pb_2(CO_3)(OH)_2$	0.14	1.49

three distinctive C═O stretches at 1382, 1462, and 1542 cm^{-1} and a broad band at ~3355 cm^{-1} due to O−H stretching. Similarly for [**Cu**], the three C═O stretching vibrations are observed at 1389 and 1499 cm^{-1}, while the broad O−H stretching bands are observed at 3320 and 3407 cm^{-1}. The infrared spectra exhibit three strong bands at 1450, 1563, and 1605 cm^{-1} for [**Ni**] and 1350, 1392, and 1637 cm^{-1} for [**Pb**] in addition to a broad band at 3272 cm^{-1} for [**Ni**] and 3536 cm^{-1} for [**Pb**].

Thermal behaviors of compounds recorded up to 600 °C indicate that all of samples are stable up to around 250 °C and the data is given in Figure 4. All samples except [**Mg**] exhibit one-step behavior resulting from decomposition at high temperatures according to the following equation

$$M(CO_3)_x(OH)_{2-2x} \rightarrow MO(s) + xCO_2(g) + (1-x)H_2O(g)$$

The decomposition reaction also shows that the weight loss is due to the formation of H_2O and CO_2 molecules. The two-step decomposition behavior of [**Mg**] could be attributed to the removal of H_2O molecules present in the molecular formula in the first step followed by a similar decomposition to other minerals in the second step.

dx.doi.org/10.1021/la201569m |*Langmuir* 2011, 27, 10642–10647

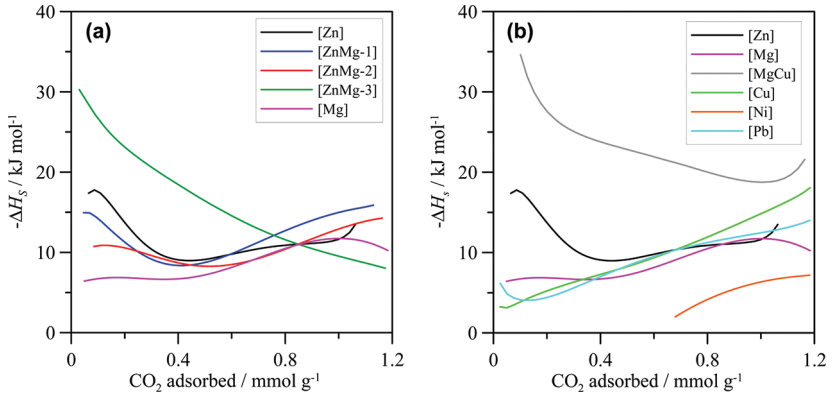

Figure 6. Isosteric heats of adsorption, ΔH_s, of CO_2 on compounds studied in this work.

3.2. CO_2 Sorption Studies. The CO_2 adsorption−desorption profile for each hydroxy metal carbonate was determined by exposing the sample to increasing and decreasing pressure increments of CO_2 gas at specific temperatures followed by evacuation.[35] The sample and gas were allowed to come to equilibrium at each pressure point. The corresponding weight change was then corrected for buoyancy to obtain the adsorption amount (mmol of CO_2/g of adsorbent). Activated carbon (Norit RB3 extra) was used for calibration purposes (see Experimental Section).

Gravimetric CO_2 capacities are determined at 316 K and pressures up to 175 bar are shown in Figure 5. Additional isotherms such as 325, 334, and 343 K are displayed in the Supporting Information. The CO_2 adsorption isotherm of [**Pb**] exhibits "type IV" behavior while the other samples exhibit "type V" behavior. Nullaginite ([**Ni**]) mineral exhibits the highest CO_2 adsorption (~1.72 mmol CO_2/g adsorbent at 175 bar and 43 °C), while mcguinnessite ([**CuMg-1**]) exhibits the highest adsorption at lower pressures (~0.8 mmol CO_2/g adsorbent at 35 bar and 316 K) (Table 2). It was also observed that the adsorption amount increases as the magnesium amount increases in the hydrozincite series. Desorption profiles are not displayed for clarity sake, since no hysteresis was observed.

3.3. Heat of Adsorption. The isosteric heat of adsorption, ΔH_s, was calculated to further understand the adsorption properties of the studied solids. ΔH_s was obtained from experimental adsorption isotherms using the Clausius−Clapeyron equation. Experimental adsorption isotherms have to be converted to calculated isosteric adsorption ΔH_s. Fitting of experimental adsorption isotherms to Freundlich, Langmuir−Freundlich, and double site Langmuir−Freundlich models led to large deviations with experimental results. Therefore, it was fitted to a rational type empirical equation (eq 2), which led to accurate correlations of experimental results:

$$p = \frac{a + cQ + eQ^2 + gQ^3}{1 + bQ + dQ^2 + fQ^3 + hQ^4} \qquad (2)$$

where a−f are fitting parameters, and Q is the amount of adsorbed CO_2. Calculated ΔH_s values are reported in Figure 6. Reported results shows moderate ΔH_s values in the 5−20 kJ mol^{-1} range, with the exception of [**ZnMg-3**] and [**MgCu**] compounds, which show ΔH_s > 20 kJ mol^{-1}, especially for low loadings. These moderate ΔH_s values point to weak CO_2−adsorbent interactions, which would lead to easy regeneration and reuse of these absorbents through multiple adsorption−desorption cycles. The behavior of bimetallic studied solids is complex; a comparison of the effect of metal ratios for Zn:Mg compounds is shown in Figure 6a. Results show that ΔH_s decreases with increasing load for these Zn:Mg compounds, reaching an almost constant value for the higher loads. The ΔH_s value at low loads shows that the CO_2−adsorbate affinity evolves in the order [**Zn**] > [**ZnMg-1**] > [**ZnMg-2**] > [**Mg**], with the anomalous behavior of [**ZnMg-3**] bimetallic solid. Nevertheless, values at high loads (high pressures) show small differences for all the Zn:Mg bimetallic solids. A comparison between solids containing the studied metals is reported in Figure 6b. Results show remarkably large ΔH_s values for the [**MgCu**] bimetallic solid, which are larger than [**Mg**] and [**Cu**] solids, and thus, mixed metal solids seem to lead to an increase of CO_2−adsorbent affinity, as it is reported in Figure 6a,b for [**ZnMg-3**] and [**MgCu**]. [**Ni**] has the lowest ΔH_s among the studied solids, in spite of leading to the largest CO_2 adsorptions at high pressure; this is probably a consequence of the large fraction of defects in this solid inferred from the broad Bragg peaks reported in previous sections. Low load ΔH_s and thus CO_2−absorbate affinity follow the order [**Zn**] > [**Mg**] > [**Pb**] > [**Cu**] > [**Ni**], whereas values for high loads are very similar for all the studied solids, with the exception of [**Ni**].

4. CONCLUSIONS

Several hydroxy metal carbonate samples were successfully prepared with a conventional precipitation method followed by a filtration and drying process. The structures of these samples were matched with corresponding minerals using powder X-ray diffraction analysis. The metal composition in bimetallic carbonates was determined with ICP-OES analysis.

The CO_2 adsorption measurements were performed at four different temperatures (316, 325, 334, and 343 K) up to high pressures (175 bar) using a Rubotherm magnetic suspension balance. Of these, nullaginite ([**Ni**]) mineral exhibits the highest CO_2 adsorption (~1.72 mmol CO_2/g adsorbent at 175 bar and 316 K). Isosteric heat of adsorption data show moderate CO_2−adsorbate affinity, which increases for bimetallic compounds in comparison with single metallic solids.

■ ASSOCIATED CONTENT

Supporting Information. Adsorption−desorption profiles of hydroxy metal carbonates from high-pressure magnetic suspension sorption apparatus between 316 and 343 K up to 175 bar.

This material is available free of charge via the Internet at http://pubs.acs.org/.

AUTHOR INFORMATION

Corresponding Author
*E-mail: mert.atilhan@qu.edu.qa.

ACKNOWLEDGMENT

This paper was made possible by the support of an NPRP grant (No: NPRP-08-670-1-124) from the Qatar National Research Fund. We also grateful for the support from NSF grant DMR-0805148. The statements made herein are solely the responsibility of the authors.

REFERENCES

(1) Yang, H. Q.; Xu, Z. H.; Fan, M. H.; Gupta, R.; Slimane, R. B.; Bland, A. E.; Wright, I. *J. Environ. Sci.* **2008**, *20*, 14.
(2) Desideri, U.; Paolucci, A. *Energy Convers. Manage.* **1999**, *40*, 1899.
(3) Keith, D. W.; Ha-Duong, M.; Stolaroff, J. K. *Clim. Change* **2006**, *74*, 17.
(4) Song, C. S. *Catal. Today* **2006**, *115*, 2.
(5) Yamasaki, A. *J. Chem. Eng. Jpn.* **2003**, *36*, 361.
(6) Rao, A. B.; Rubin, E. S. *Environ. Sci. Technol.* **2002**, *36*, 4467.
(7) Karadas, F.; Atilhan, M.; Aparicio, S. *Energy Fuels* **2010**, *24*, 5817.
(8) Siriwardane, R. W.; Shen, M.-S.; Fisher, E. P. *Energy Fuels* **2005**, *19*, 1153.
(9) Furukawa, H.; Yaghi, O. M. *J. Am. Chem. Soc.* **2009**, *131*, 8875.
(10) Barton, T. J.; Bull, L. M.; Klemperer, W. G.; Loy, D. A.; McEnaney, B.; Misono, M.; Monson, P. A.; Pez, G.; Scherer, G. W.; Vartuli, J. C.; Yaghi, O. M. *Chem. Mater.* **1999**, *11*, 2633.
(11) Sridhar, S.; Smitha, B.; Aminabhavi, T. M. *Sep. Purif. Rev.* **2007**, *36*, 113.
(12) Lee, J.-S.; Kim, J.-H.; Kim, J.-T.; Suh, J.-K.; Lee, J.-M.; Lee, C.-H. *J. Chem. Eng. Data* **2002**, *47*, 1237.
(13) Drage, T. C.; Kozynchenko, O.; Pevida, C.; Plaza, M. G.; Rubiera, F.; Pis, J. J.; Snape, C. E.; Tennison, S. *Energy Procedia* **2009**, *1*, 599.
(14) Cazorla-Amorós, D.; Alcañiz-Monge, J.; Linares-Solano, A. *Langmuir* **1996**, *12*, 2820.
(15) Goetz, V.; Pupier, O.; Guillot, A. *Adsorption* **2006**, *12*, 55.
(16) Himeno, S.; Komatsu, T.; Fujita, S. *J. Chem. Eng. Data* **2005**, *50*, 369.
(17) Belmabkhout, Y.; Serna-Guerrero, R.; Sayari, A. *Ind. Eng. Chem. Res.* **2010**, *49*, 359.
(18) He, Y.; Seaton, N. A. *Langmuir* **2006**, *22*, 1150.
(19) Belmabkhout, Y.; Serna-Guerrero, R.; Sayari, A. *Chem. Eng. Sci.* **2009**, *64*, 3721.
(20) D'Alessandro, D. M.; Smit, B.; Long, J. R. *Angew. Chem. Int. Ed* **2010**, *49*, 6058.
(21) Choi, S.; Drese, J. H.; Jones, C. W. *ChemSusChem* **2009**, *2*, 796.
(22) Cavenati, S.; Grande, C. A.; Rodrigues, A. E. *J. Chem. Eng. Data* **2004**, *49*, 1095.
(23) Dreisbach, F.; Staudt, R.; Keller, J. U. *Adsorption* **1999**, *5*, 215.
(24) Millward, A. R.; Yaghi, O. M. *J. Am. Chem. Soc.* **2005**, *127*, 17998.
(25) Nelson, T. O.; Coleman, L. J. I.; Green, D. A.; Gupta, R. P. *Energy Procedia* **2009**, *1*, 1305.
(26) Keith, D. W.; Minh, H.-D.; Stolaroff, J. K. *Clim. Change* **2006**, *74*, 17.
(27) Dreisbach, F.; Lösch, H. W. *J. Thermal Anal. Calorim.* **2000**, *62*, 515.
(28) Roberts, W. L.; Campbell, T. J.; Rapp Jr., G. R. *Encyclopedia of Minerals*, 2nd ed.; Chapman & Hall: New York, 1990.
(29) Hales, M. C.; Frost, R. L. *Polyhedron* **2007**, *26*, 4955.
(30) Han, H.; Hu, S.; Feng, J.; Gao, H. *Appl. Surf. Sci.* **2011**, *257*, 2677.
(31) Frost, R. L.; Wain, D. L.; Martens, W. N.; Reddy, B. J. *Polyhedron* **2007**, *26*, 275.
(32) Koga, N.; Criado, J. M.; Tanaka, H. *Thermochim. Acta* **1999**, *340−341*, 387.
(33) Bucca, M.; Dietzel, M.; Tang, J.; Leis, A.; Köhler, S. J. *Chem. Geol.* **2009**, *266*, 143.
(34) Nickel, E. H.; Hallbert, J. A.; Halligan, R. *Geol. Soc. Aust.* **1979**, *26*, 61.
(35) Yang, R. T. *Adsorbents: Fundamentals and Applications*; John Wiley & Sons Inc.: New York, 2003.